A new *in vivo* model to analyze hepatic metastasis of the human colon cancer cell line HCT116 in NOD/Shi-*scid*/IL-2Rγ^{null} (NOG) mice by ^{18}F-FDG PET/CT

KENJI KAWAI[1], KATSUMI TAMURA[3], IKUKO SAKATA[3], JIRO ISHIDA[3], MASAYOSHI NAGATA[4], HIDEO TSUKADA[5], HIROSHI SUEMIZU[2], MASATO NAKAMURA[1,6], YOSHIYUKI ABE[3] and TSUYOSHI CHIJIWA[1]

[1]Pathology Research Department, [2]Biomedical Research Department, Central Institute for Experimental Animals, Kawasaki, Kanagawa 210-0821; [3]Tokorozawa PET Diagnostic Imaging Clinic, Tokorozawa, Saitama 359-1124; [4]Iruma Heart Hospital, Iruma, Saitama 358-0026; [5]Central Research Laboratory, Hamamatsu Photonics K.K., Hamamatsu, Shizuoka 434-8601; [6]Department of Regenerative Medicine and Pathology, Tokai University School of Medicine, Isehara, Kanagawa 259-1193, Japan

Received September 10, 2012; Accepted October 23, 2012

DOI: 10.3892/or.2012.2141

Abstract. Clinically, ^{18}F-fluorodeoxyglucose positron emission tomography/computed tomography (^{18}F-FDG-PET/CT) is useful in the evaluation of various types of human cancers. While PET analysis has been established to evaluate subcutaneous lesions of human cancers in mice, its applications for internal lesions are still being developed. We are currently evaluating new PET approaches for the effective evaluation of *in vivo* metastatic lesions in the internal organs of small experimental animals. In this study, we analyzed *in vivo* hepatic metastases of human colonic cancer in immunodeficient mice (NOD/Shi-*scid*/IL-2Rγ^{null}, NOG) using PET imaging. This new PET approach has been proposed for the evaluation of *in vivo* metastatic lesions in internal organs. The human colon cancer line HCT116 ($1.0x10^5$ and $1.0x10^6$ cells/mouse) was transplanted by intrasplenic injection. ^{18}F-FDG-PET/CT scans were performed 2 weeks after transplantation. After PET/CT scans, histopathological examinations were performed. PET/CT analysis disclosed multiple metastatic foci and increased standardized uptake values (SUV) of FDG in the livers of NOG mice (control, SUVmean 0.450±0.033, SUVmax 0.635±0.017; $1.0x10^5$ cells, 0.853±0.087, 1.254±0.237; $1.0x10^6$ cells, 1.211±0.108, 1.701±0.158). There were significant differences in FDG uptakes between the three groups (ANOVA, P=0.017 in SUVmean; P=0.044 in SUVmax, n=2). We clearly and quantitatively detected images of hepatic metastasis in the livers of NOG mice by ^{18}F-FDG-PET/CT *in vivo*. PET/CT analysis of internal organ lesions of human cancerous xenografts is a new reliable experimental system to simulate metastases. This model system is useful for analyzing metastatic mechanisms and for developing new novel drugs targeting hepatic metastases of cancer.

Correspondence to: Dr Tsuyoshi Chijiwa, Pathology Research Department, Central Institute for Experimental Animals, 3-25-12 Tonomachi, Kawasaki-ku, Kawasaki, Kanagawa 210-0821, Japan
E-mail: chijiwa@ciea.or.jp

Key words: ^{18}F-FDG, PET, NOG mouse, colon cancer, tumor xenograft

Introduction

Chemotherapy has contributed to improvements in the outcome of colorectal cancer (1,2), yet the control of metastatic lesions is crucial for improving outcomes. The metastatic mechanisms of colon cancer are still not known in detail; however, previous studies by us and others have identified the key molecules related to liver metastasis in colon cancer (3-5), and pathological findings of budding and venous invasion of tumors are known to be important in predicting the outcome of colorectal cancer (6,7). Clinically, ^{18}F-fluorodeoxyglucose positron emission tomography/computed tomography (^{18}F-FDG-PET/CT) fusion imaging is a useful tool for evaluating the stage, recurrence, outcome, and effectiveness of treatment in human cancers (8-11). Some studies have reported that PET/CT is useful in colon cancer (12-14). However, PET/CT imaging has a limitation in revealing hepatic metastasis due to normal uptake in the liver (15).

Many studies have shown that *in vivo* studies with subcutaneous xenografts in nude mice and severe combined immunodeficient (SCID) mice are useful for analyzing human cancers (16-19), whereas they are limited in evaluating internal organ metastases associated with human cancers. Immunodeficient mice commonly show poor metastatic lesions *in vivo*. We reported that distant metastatic lesions were easily reproduced by human cancer cell lines in newly developed NOD/Shi-*scid*/IL-2Rγ^{null} (NOG) mouse models employing systemic injections (20-23). It was confirmed that

the experimental metastasis model of human cancer using NOG mice was more sensitive and easier to achieve than that using SCID mice due to their multiple immunological dysfunctions not only in cytokine production capability, but also in the functional competence of T, B and NK cells (24,25). We previously developed a reliable new model for assaying hepatic metastasis with superimmunodeficient NOG mice (26,27).

Some *in vivo* studies have evaluated metastatic lesions of internal organs in mice with conventional modalities such as bio-luminescence imaging (BLI), but difficulties were found in revealing the mechanisms of metastasis (28). Therefore, a new *in vivo* system to detect internal organ metastatic lesions is required to simulate the clinical situation of metastatic lesions using reliable and quantitative approaches.

In this study, we examined whether ^{18}F-FDG-PET/CT scans could semi-quantitatively reveal abnormal FDG uptakes in hepatic metastasis of human colon cancer cell line HCT116 in NOG mice, thereby overcoming the above described limitations encountered when evaluating metastatic lesions in the liver. Moreover, liver metastasis in NOG mice was studied by histopathological analysis. We showed here that the evaluation of metastatic lesions in NOG mice by PET/CT may be an extremely useful *in vivo* metastatic model.

Materials and methods

Cell culture. The HCT116 cell line was obtained from the American Type Culture Collection (Manassas, VA, USA) and maintained in McCoy's 5A medium (Sigma-Aldrich, St. Louis, MO, USA) supplemented with 10% heat-inactivated fetal bovine serum, 100 U/ml penicillin and 100 μg/ml streptomycin. Cells were incubated in a humidified (37˚C, 5% CO_2) incubator and passaged on reaching 80% confluence.

In vivo transplantation of human colon cancer cell line, HCT116. NOG mice (9-12 weeks of age, male) were maintained at the specific pathogen-free facilities of the Central Institute for Experimental Animals (CIEA, Kawasaki, Japan). Experimental liver metastases using NOG mice were generated by intrasplenic injection of HCT116 cells ($1.0x10^5$ and $1.0x10^6$/mouse, n=2) and splenectomy. All experiments involving laboratory animals were performed in accordance with the care and use guidelines of the CIEA, according to our previous reports (26,27).

Whole-body imaging of NOG mice with ^{18}F-FDG-PET and CT scans. Positron-emitting fluorine-18 (^{18}F) was produced by ^{18}O(p,n)^{18}F nuclear reaction using a cyclotron (HM-18; Sumitomo Heavy Industry, Osaka, Japan) at Hamamatsu Photonics PET Center. ^{18}F-FDG-PET and CT scans were performed in NOG mice 14 days after transplantation. The production of ^{18}F-FDG was carried out according to a method described elsewhere (29). The kinetics and distribution patterns of the radiolabeled compound were determined with a small animal PET scanner (ClairvivoPET; Shimadzu Corp., Kyoto, Japan). This scanner consists of depth of interaction (DOI) detector modules with an axial field of view (FOV) of 151 mm, a transaxial FOV of 102 mm, and a transaxial spatial resolution of 1.54 mm in the center (30). Anesthetized mice were placed in a prone position on a fixation plate and then placed in the gantry hole of the PET scanner. After transmission measurement with an external ^{137}Cs point source (22 MBq) for attenuation correction, ^{18}F-FDG at a dose of 6 MBq (0.2 ml) was injected intravenously into each mouse via the tail vein. Data were acquired in list-mode format for 60 min; full 3D sinograms with corrected efficiency, scattering, attenuation, count losses and decay were reconstructed using an iterative 3D dynamic raw-action maximum likelihood algorithm (Drama). Summation images from 40 to 60 min after ^{18}F-FDG injection were reconstructed, and average and maximum values of the standardized uptake (SUVmean, SUVmax) were semi-quantitatively calculated in various organs of NOG mice. After PET scanning, a CT scan was performed with ClairvivoCT (Shimadzu Corp.) in each NOG mouse.

Table I. SUV values in the various organs of control NOG mice by ^{18}F-FDG-PET/CT.

	SUVmean	SUVmax
Brain	1.519±0.083	2.140±0.127
Heart	1.343±0.035	1.868±0.016
Kidney	2.163±0.125	3.148±0.150
Bladder	32.986±3.590	49.692±8.152
Lung	0.577±0.064	1.384±0.104
Liver	0.450±0.033	0.635±0.017
Muscle	0.151±0.011	0.327±0.040
Bone	0.214±0.013	0.476±0.034
Intestine	0.824±0.033	2.061±0.111
Testis	0.510±0.022	1.212±0.335

Standardized uptake values (SUV) were examined by ^{18}F-FDG.

Macroscopic and microscopic examinations. Mice were autopsied after PET/CT scan examinations to evaluate liver metastases. These metastatic lesions were also histologically confirmed. Immunohistochemistry was carried out on 4 μm tissue sections using the Bond Polymer Refine Detection system (Leica Microsystems, Tokyo, Japan) according to the manufacturer's instructions with minor modifications. In brief, 4 μm sections of formalin-fixed, paraffin-embedded tissues were deparaffinized by Bond Dewax Solution (Leica Microsystems) and an antigen retrieval procedure was carried out using Bond ER solution (Leica Microsystems) for 30 min at 100˚C. Endogenous peroxidases were quenched by incubation with hydrogen peroxide for 5 min. Sections were incubated for 30 min at ambient temperate with primary monoclonal antibodies for anti-HLA class 1-A, B, C (Hokudo, Sapporo, Japan) using the biotin-free polymeric horseradish peroxidase (HRP)-linker antibody conjugate system in a Bond-Max automatic slide stainer (Leica Microsystems). Nuclei were counterstained with hematoxylin.

Statistical analysis. Statistical comparisons of data sets were analyzed by a one-way factorial ANOVA. Data are shown as means ± standard error of mean (SEM). These analyses were performed using JMP version 8 software (SAS Institute, Inc., Cary, NC, USA). P-values <0.05 were considered to indicate statistically significant differences.

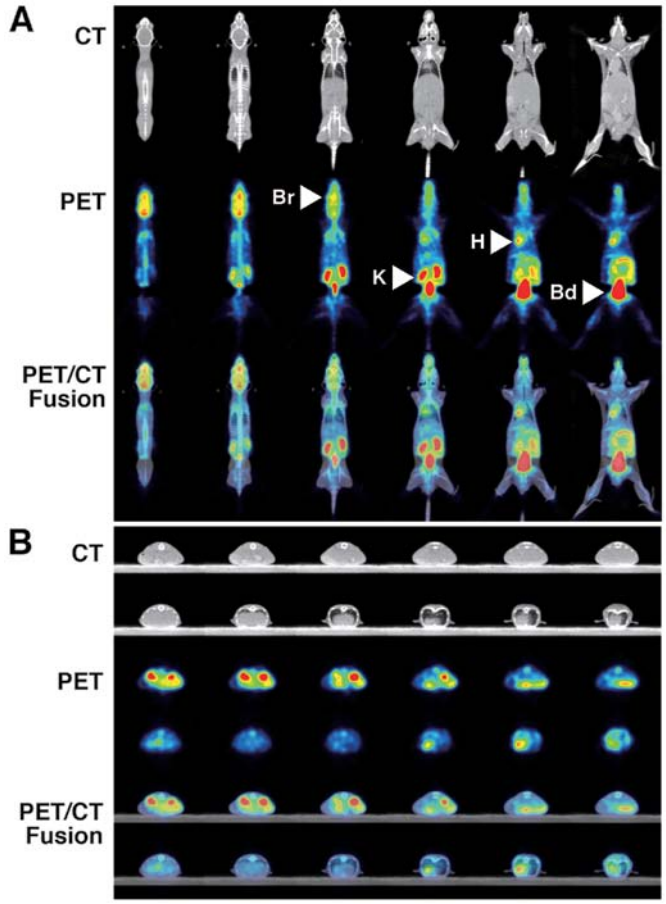

Figure 1. PET and CT findings in control NOG mice. FDG-PET/CT shows intense FDG uptakes in the brain (Br, SUVmax 2.140±0.127), heart (H, SUVmax 1.868±0.016), kidney (K, SUVmax 3.148±0.150) and bladder (Bd, SUVmax 49.692±8.152) of control NOG mice. (A) Coronal view, (B) axial view. Upper panels, CT; middle panels, PET; lower panels, PET/CT fusion.

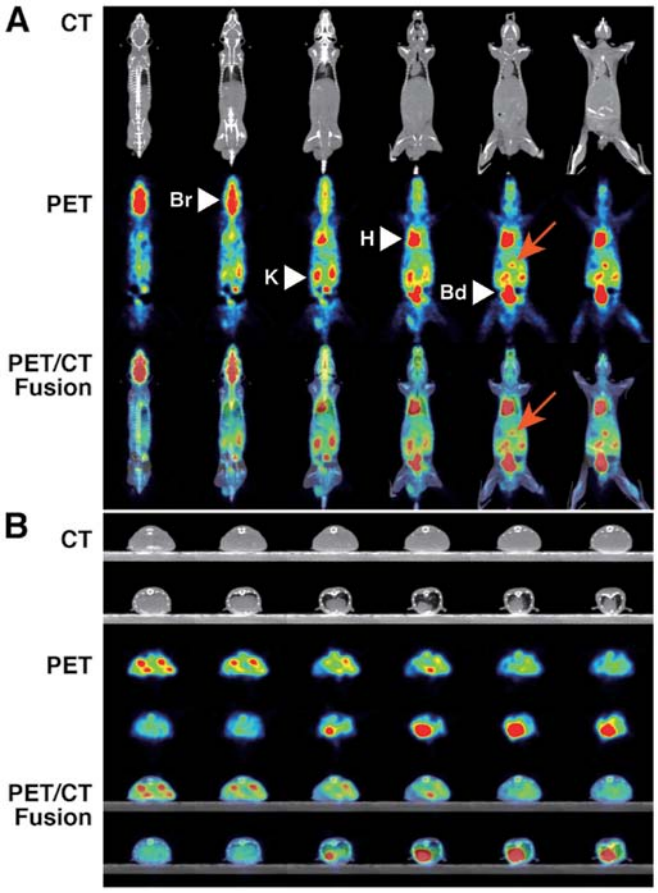

Figure 2. PET and CT findings in NOG mice transplanted with $1.0x10^5$ of HCT116 cells. FDG-PET/CT shows significantly increased multiple FDG uptakes (red arrow, SUVmax 1.017) in the livers of NOG mice transplanted with $1.0x10^5$ cells of the HCT116 cell line. (A) Coronal view, (B) axial view. Upper panels, CT; middle panels, PET; lower panels, PET/CT fusion. Br, brain; H, heart; K, kidney; Bd, bladder.

Results

^{18}F-FDG-PET findings in control NOG mice. ^{18}F-FDG-PET/CT showed intense FDG uptakes in the brain (SUVmean 1.519±0.083, SUVmax 2.140±0.127), heart (SUVmean 1.343±0.035, SUVmax 1.868±0.016), kidney (SUVmean 2.163±0.125, SUVmax 3.148±0.150) and bladder (SUVmean 32.986±3.590, SUVmax 49.692±8.152) of control NOG mice (Table I, Fig. 1).

^{18}F-FDG-PET and CT findings of tumor metastasis in NOG mice. ^{18}F-FDG-PET/CT showed higher multiple FDG uptakes (SUVmean 0.853±0.087, SUVmax 1.254±0.237) in the livers of NOG mice transplanted with $1.0x10^5$ cells of the HCT116 cell line (Table II, Fig. 2) than those of control NOG mice (SUVmean 0.450±0.033, SUVmax 0.635±0.017). CT scans also showed marked liver swelling in NOG mice transplanted with $1.0x10^6$ cells of HCT116 (Fig. 3). PET/CT showed diffuse higher FDG uptakes (SUVmean 1.211±0.108, SUVmax 1.701±0.158) in the livers of NOG mice with injection of $1.0x10^6$ HCT116 cells than FDG uptakes with $1.0x10^5$ cells. There were significant differences in FDG uptakes between the three groups (ANOVA, P=0.017 in SUVmean, P=0.044 in SUVmax). No other organs with abnormal FDG uptake were noted besides that of the livers of NOG mice transplanted with $1.0x10^5$ and $1.0x10^6$ cells of HCT116.

Table II. SUV values in the livers of NOG mice by ^{18}F-FDG-PET/CT.

	SUVmean	SUVmax
Control	0.450±0.033[a]	0.635±0.017[b]
$1.0x10^5$ cells of HCT116	0.853±0.087[a]	1.254±0.237[b]
$1.0x10^6$ cells of HCT116	1.211±0.108[a]	1.701±0.158[b]

Standardized uptake values (SUV) were examined by ^{18}F-FDG-PET/CT. ANOVA, [a]P=0.017, [b]P=0.044; n=2.

In vivo liver metastasis. Experimental liver metastases, which consisted of solid white masses, were detected in all livers of NOG mice transplanted with $1.0x10^5$ and $1.0x10^6$ cells of the HCT116 cell line. Metastatic hepatomegaly transplanted with $1.0x10^6$ cells was more severe than that with $1.0x10^5$ cells (Fig. 4, H&E). It was also immunohistochemically confirmed that there were obviously more metastatic foci in the livers of

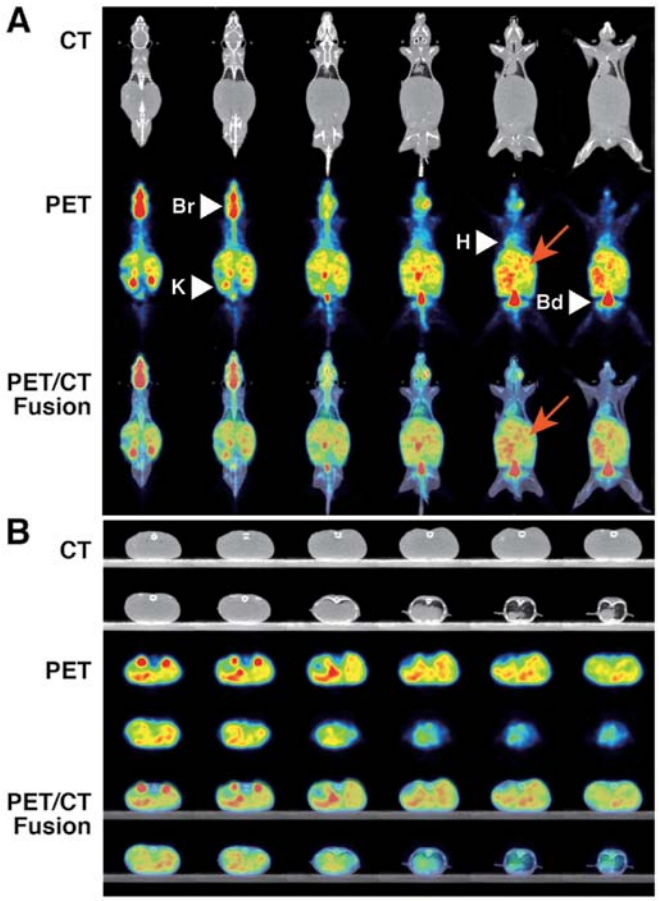

Figure 3. PET and CT findings in NOG mice transplanted with $1.0x10^6$ of HCT116 cells. CT scans show marked liver swelling in NOG mice transplanted with $1.0x10^6$ of HCT116 cells. PET/CT show diffuse higher FDG uptakes (red arrow, SUVmax 1.859) in livers. (A) Coronal view, (B) axial view. Upper panels, CT; middle panels, PET; lower panels, PET/CT fusion. Br, brain; H, heart; K, kidney; Bd, bladder.

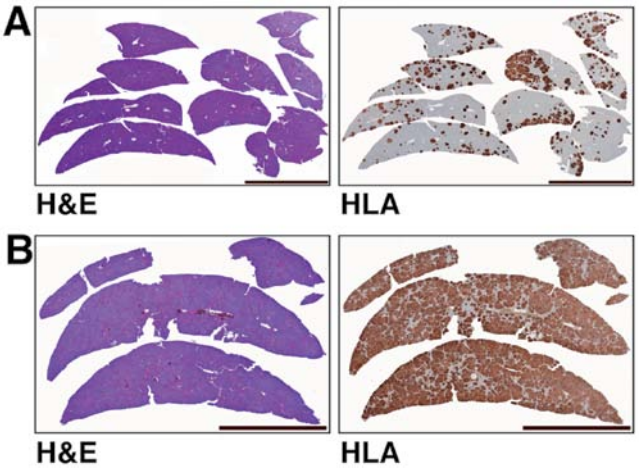

Figure 4. Histopathological findings of liver metastases. Experimental liver metastases in mice transplanted with both $1.0x10^5$ and $1.0x10^6$ of HCT116 cells showed metastatic hepatomegaly. Anti-HLA immunohistochemical examinations revealed that there were many more metastatic foci of human cancer in the livers of NOG mice transplanted with $1.0x10^6$ than foci in mice transplanted with $1.0x10^5$ of HCT116 cells. (A) $1.0x10^5$ HCT116 cells, (B) $1.0x10^6$ HCT116 cells; H&E, hematoxylin and eosin; HLA, anti-HLA immunohistochemistry; Scale bar, 5 mm.

NOG mice transplanted with $1.0x10^6$ than in mice transplanted with $1.0x10^5$ HTC116 cells (Fig. 4, HLA).

Discussion

In this study, we clearly and quantitatively demonstrated increased multiple ^{18}F-FDG uptakes in hepatic metastases of human colonic cancer cell line HCT116 in NOG mouse models using a small animal PET/CT system. We previously reported that ^{18}F-FDG-PET/CT clinically is a very useful imaging modality to evaluate human cancers, including rare carcinoma cases (31-34). Many reports have shown that animal PET imaging is useful for evaluating human cancer xenografts *in vivo*. It is usually difficult to reveal metastases as conventional *in vivo* models are limited in their evaluation of metastases associated with human cancers (28,35). It is easy to produce experimental liver metastases in immunocompromised NOG mice because of their multiple immunological dysfunctions in cytokine production capability as well as functional competence of T, B and NK cells (24-27). However, quantitative evaluation of experimental liver metastases is still being developed. We previously reported the use of liver weight as an index of metastatic hepatomegaly or microvessel counts to reflect tumor cell activity (23,36). We present herein that the model system with NOG mice and a small animal PET/CT system has the feasibility of a quantitative metastasis model to simulate clinical situations. Several studies have reported the development of new anticancer therapies and novel drugs for human cancers using animal PET (37,38). This model system presented here with NOG mice and a small animal PET/CT system may be useful for developing new anticancer therapies and novel drugs for hepatic metastases of human cancers.

Although PET imaging with ^{18}F-FDG is routinely used for tumor detection and therapy monitoring, several limitations have been reported with ^{18}F-FDG, such as high uptake in normal tissues of the brain and inflammatory tissues (15,39). In contrast, positron-labeled amino acids and their analogs are considered to be useful because of the low rate of amino acid use in normal control tissues. Natural and unnatural artificial labeled amino acids have been reported (40,41). This hepatic metastasis model, using intrasplenic injection of small numbers of cancer cells into NOG mice, is reliable and quantitative, and more closely mimics *in vivo* conditions (26). New compounds, which are more sensitive and specific for the detection of human cancers, are expected to replace ^{18}F-FDG (42,43). The hepatic metastasis model system in NOG mice combined with small animal PET/CT analysis will be useful in developing new labeling compounds for PET.

In conclusion, the hepatic metastasis model system in NOG mice combined with PET/CT has the feasibility to simulate clinical situations, and this model system is useful for analyzing mechanisms of metastasis and developing new therapeutic approaches for metastatic lesions of human cancers.

Acknowledgements

We are grateful to Hiroshi Iwata, Takeharu Kaiuchi, Norihiro Harada and Dai Fukumoto for their technical assistance and helpful discussions.

References

1. O'Connor ES, Greenblatt DY, LoConte NK, *et al*: Adjuvant chemotherapy for stage II colon cancer with poor prognostic features. J Clin Oncol 29: 3381-3388, 2011.
2. Karoui M, Roudot-Thoraval F, Mesli F, *et al*: Primary colectomy in patients with stage IV colon cancer and unresectable distant metastases improves overall survival: results of a multicentric study. Dis Colon Rectum 54: 930-938, 2011.
3. Tokunaga T, Oshika Y, Abe Y, *et al*: Vascular endothelial growth factor (VEGF) mRNA isoform expression pattern is correlated with liver metastasis and poor prognosis in colon cancer. Br J Cancer 77: 998-1002, 1998.
4. Tokunaga T, Nakamura M, Oshika Y, *et al*: Thrombospondin 2 expression is correlated with inhibition of angiogenesis and metastasis of colon cancer. Br J Cancer 79: 354-359, 1999.
5. Sun L, Hu H, Peng L, *et al*: P-cadherin promotes liver metastasis and is associated with poor prognosis in colon cancer. Am J Pathol 179: 380-390, 2011.
6. Tanaka M, Hashiguchi Y, Ueno H, Hase K and Mochizuki H: Tumor budding at the invasive margin can predict patients at high risk of recurrence after curative surgery for stage II, T3 colon cancer. Dis Colon Rectum 46: 1054-1059, 2003.
7. Sato T, Ueno H, Mochizuki H, *et al*: Objective criteria for the grading of venous invasion in colorectal cancer. Am J Surg Pathol 34: 454-462, 2010.
8. Cronin CG, Swords R, Truong MT, *et al*: Clinical utility of PET/CT in lymphoma. Am J Roentgenol 194: W91-W103, 2010.
9. Ueda S, Saeki T, Shigekawa T, *et al*: ^{18}F-fluorodeoxyglucose positron emission tomography optimizes neoadjuvant chemotherapy for primary breast cancer to achieve pathological complete response. Int J Clin Oncol 17: 276-282, 2012.
10. Xie L, Saynak M, Veeramachaneni NK, *et al*: Non-small cell lung cancer: prognostic importance of positive FDG PET findings in the mediastinum for patients with N0-N1 disease at pathologic analysis. Radiology 261: 226-234, 2011.
11. Abe Y, Tamura K, Sakata I, *et al*: Clinical implications of 18F-fluorodeoxyglucose positron emission tomography/computed tomography at delayed phase for diagnosis and prognosis of malignant pleural mesothelioma. Oncol Rep 27: 333-338, 2012.
12. Mori S and Oguchi K: Application of (18)F-fluorodeoxyglucose positron emission tomography to detection of proximal lesions of obstructive colorectal cancer. Jpn J Radiol 28: 584-590, 2010.
13. Ducreux M and Dromain C: Non-invasive imaging tools in colorectal cancer. Rev Prat 60: 1071-1073, 2010 (In French).
14. Treglia G, Calcagni ML, Rufini V, *et al*: Clinical significance of incidental focal colorectal (18)F-fluorodeoxyglucose uptake: our experience and a review of the literature. Colorectal Dis 14: 174-180, 2012.
15. Kubota R, Kubota K, Yamada S, Tada M, Ido T and Tamahashi N: Microautoradiographic study for the differentiation of intratumoral macrophages, granulation tissues and cancer cells by the dynamics of fluorine-18-fluorodeoxyglucose uptake. J Nucl Med 35: 104-112, 1994.
16. Abe Y, Nakamura M, Ohnishi Y, Inaba M, Ueyama Y and Tamaoki N: Multidrug resistance gene (MDR1) expression in human tumor xenografts. Int J Oncol 5: 1285-1292, 1994.
17. Abe Y, Ohnishi Y, Yoshimura M, *et al*: P-glycoprotein-mediated acquired multidrug resistance of human lung cancer cells in vivo. Br J Cancer 74: 1929-1934, 1996.
18. Suto R, Abe Y, Nakamura M, *et al*: P-glycoprotein-mediated acquired multidrug resistance of human osteosarcoma xenografts *in vivo*. Int J Oncol 12: 287-291, 1998.
19. Fujimori S, Abe Y, Nishi M, *et al*: The subunits of glutamate cysteine ligase enhance cisplatin resistance in human non-small cell lung cancer xenografts *in vivo*. Int J Oncol 25: 413-418, 2004.
20. Miyakawa Y, Ohnishi Y, Tomisawa M, *et al*: Establishment of a new model of human multiple myeloma using NOD/SCID/gamma(c)(null) (NOG) mice. Biochem Biophys Res Commun 313: 258-262, 2004.
21. Ikoma N, Yamazaki H, Abe Y, *et al*: S100A4 expression with reduced E-cadherin expression predicts distant metastasis of human malignant melanoma cell lines in the NOD/SCID/γ_C^{null} (NOG) mouse model. Oncol Rep 14: 633-637, 2005.
22. Hamada K, Monnai M, Kawai K, *et al*: Liver metastasis models of colon cancer for evaluation of drug efficacy using NOD/Shi-scid IL2Rγ^{null} (NOG) mice. Int J Oncol 32: 153-159, 2008.
23. Chijiwa T, Abe Y, Ikoma N, *et al*: Thrombospondin 2 inhibits metastasis of human malignant melanoma through microenvironment-modification in NOD/SCID/γ_C^{null} (NOG) mice. Int J Oncol 34: 5-13, 2009.
24. Ito M, Hiramatsu H, Kobayashi K, *et al*: NOD/SCID/gamma(c)(null) mouse: an excellent recipient mouse model for engraftment of human cells. Blood 100: 3175-3182, 2002.
25. Hiramatsu H, Nishikomori R, Heike T, *et al*: Complete reconstitution of human lymphocytes from cord blood CD34$^+$ cells using the NOD/SCID/gamma(c)(null) mice model. Blood 102: 873-880, 2003.
26. Suemizu H, Monnai M, Ohnishi Y, Ito M, Tamaoki N and Nakamura M: Identification of a key molecular regulator of liver metastasis in human pancreatic carcinoma using a novel quantitative model of metastasis in NOD/SCID/γ_c^{null} (NOG) mice. Int J Oncol 31: 741-751, 2007.
27. Kubo A, Ohmura M, Wakui M, *et al*: Semi-quantitative analyses of metabolic systems of human colon cancer metastatic xenografts in livers of superimmunodeficient NOG mice. Anal Bioanal Chem 400: 1895-1904, 2011.
28. Deroose CM, De A, Loening AM, *et al*: Multimodality imaging of tumor xenografts and metastases in mice with combined small-animal PET, small-animal CT, and bioluminescence imaging. J Nucl Med 48: 295-303, 2007.
29. Oberdorfer F, Hull WE, Traving BC and Maier-Borst W: Synthesis and purification of 2-deoxy-2-[18F]fluoro-D-glucose and 2-deoxy-2-[18F]fluoro-D-mannose: characterization of products by 1H- and 19F-NMR spectroscopy. Int J Rad Appl Instrum A 37: 695-701, 1986.
30. Mizuta T, Kitamura K, Iwata H, *et al*: Performance evaluation of a high-sensitivity large-aperture small-animal PET scanner: ClairvivoPET. Ann Nucl Med 22: 447-455, 2008.
31. Ueda S, Tsuda H, Asakawa H, *et al*: Clinicopathological and prognostic relevance of uptake level using 18F-fluorodeoxyglucose positron emission tomography/computed tomography fusion imaging (18F-FDG PET/CT) in primary breast cancer. Jpn J Clin Oncol 38: 250-258, 2008.
32. Abe Y, Tamura K, Sakata I, *et al*: Usefulness of ^{18}F-FDG positron emission tomography/computed tomography for the diagnosis of pyothorax-associated lymphoma: a report of three cases. Oncol Lett 1: 833-836, 2010.
33. Abe Y, Tamura K, Sakata I, *et al*: Unique intense uptake demonstrated by ^{18}F-FDG positron emission tomography/computed tomography in primary pancreatic lymphoma: a case report. Oncol Lett 1: 605-607, 2010.
34. Ozeki Y, Abe Y, Kita H, *et al*: A case of primary lung cancer lesion demonstrated by F-18 FDG positron emission tomography/computed tomography (PET/CT) one year after the detection of metastatic brain tumor. Oncol Lett 2: 621-623, 2011.
35. Takamiya Y, Abe Y, Tanaka Y, *et al*: Murine P-glycoprotein on stromal vessels mediates multidrug resistance in intracerebral human glioma xenografts. Br J Cancer 76: 445-450, 1997.
36. Hatanaka H, Oshika Y, Abe Y, *et al*: Vascularization is decreased in pulmonary adenocarcinoma expressing brain-specific angiogenesis inhibitor 1 (BAI1). Int J Mol Med 5: 181-183, 2000.
37. Pantaleo MA, Nicoletti G, Nanni C, *et al*: Preclinical evaluation of KIT/PDGFRA and mTOR inhibitors in gastrointestinal stromal tumors using small animal FDG PET. J Exp Clin Cancer Res 29: 173, 2010.
38. Moroz MA, Kochetkov T, Cai S, *et al*: Imaging colon cancer response following treatment with AZD1152: a preclinical analysis of [18F]fluoro-2-deoxyglucose and 3'-deoxy-3'-[18F] fluorothymidine imaging. Clin Cancer Res 17: 1099-1110, 2011.
39. Kubota K, Nakamoto Y, Tamaki N, *et al*: FDG-PET for the diagnosis of fever of unknown origin: a Japanese multi-center study. Ann Nucl Med 25: 355-364, 2011.
40. Tsukada H, Sato K, Fukumoto D, Nishiyama S, Harada N and Kakiuchi T: Evaluation of D-isomers of O-11C-methyl tyrosine and O-18F-fluoromethyl tyrosine as tumor-imaging agents in tumor-bearing mice: comparison with L- and D-11C-methionine. J Nucl Med 47: 679-688, 2006.
41. Tsukada H, Sato K, Fukumoto D and Kakiuchi T: Evaluation of D-isomers of O-18F-fluoromethyl, O-18F-fluoroethyl and O-18F-fluoropropyl tyrosine as tumour imaging agents in mice. Eur J Nucl Med Mol Imaging 33: 1017-1024, 2006.
42. Perk LR, Stigter-van Walsum M, Visser GW, *et al*: Quantitative PET imaging of Met-expressing human cancer xenografts with 89Zr-labelled monoclonal antibody DN30. Eur J Nucl Med Mol Imaging 35: 1857-1867, 2008.
43. Wang H, Liu B, Tian JH, *et al*: Monitoring early responses to irradiation with dual-tracer micro-PET in dual-tumor bearing mice. World J Gastroenterol 16: 5416-5423, 2010.